

S6-030

Structure based analysis of the magnetic resonance parameters of the phylloquinone acceptor A₁ in PS I

C Teutloff¹, R Bittl¹, M Stein¹, P Jordan², P Fromme¹, N Krauß², W Lubitz¹

¹Max-Volmer-Laboratorium, Technische Universität Berlin, Straße des 17. Juni 135, 10623 Berlin, Germany. Robert.Bittl@TU-Berlin.DE

²Institut für Chemie/Kristallographie, Freie Universität Berlin, Takustraße 6, 14195 Berlin, Germany.

Keywords: A₁, phylloquinone, EPR, ENDOR, DFT calculations

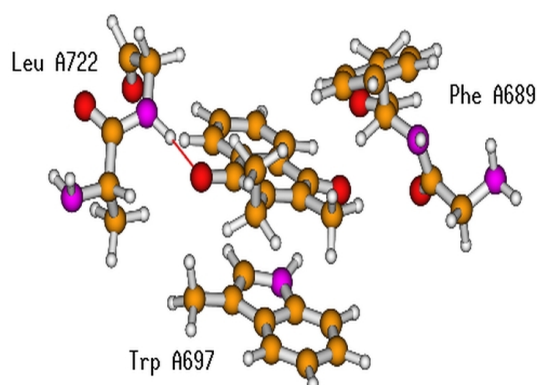
Introduction

The phylloquinone (vitamin K₁, VK₁) acceptor A₁ in photosystem I is located at the interface between electron transfer on organic cofactors and iron-sulfur clusters. To be able to reduce the F_X iron-sulfur cluster A₁ operates at a rather negative reduction potential of about -800 mV. A similar quinone, menaquinone-9, is the acceptor Q_A in the purple bacterial reaction center of *Rhodospseudomonas viridis* and acts there at a reduction potential of about -100 mV. The drastic difference in the reduction potential of such similar quinones is due to the protein environment which tunes the properties of the embedded cofactors. Sensitive probes for the protein-cofactor interaction are the magnetic resonance parameters of oxidized or reduced cofactors. The radical anion A₁^{•-} shows an altered *g* anisotropy and a modified spin density distribution compared to the VK₁^{•-} anion radical in the polar solvent isopropanol (Rigby 1996). We have measured high-field EPR and ENDOR spectra of electrochemically generated VK₁^{•-} in the non-polar solvent mixture 1,2-dimethoxy ethane/2-methyltetrahydrofuran (DME/MTHF) to obtain additional magnetic resonance parameters for this species, and performed density functional theory (DFT) calculations to correlate the observed magnetic resonance parameters of A₁^{•-} with structural elements of the A₁ binding pocket as revealed by the recently published structural model of PS I at 2.5 Å resolution (Jordan 2001).

Materials and Methods

High-field (94 GHz) EPR spectra were recorded on a BRUKER Elexsys E680 spectrometer, pulsed ENDOR spectra on a BRUKER ESP380E with a ESP360D-P

Fig 1: Model of the A₁ binding site in the PsaA subunit of PS I used for the calculations of magnetic interaction parameters. The hydrogen bond between A₁ and the backbone NH of Leu A722 is indicated ($R_{N-O} = 2.64$ Å).



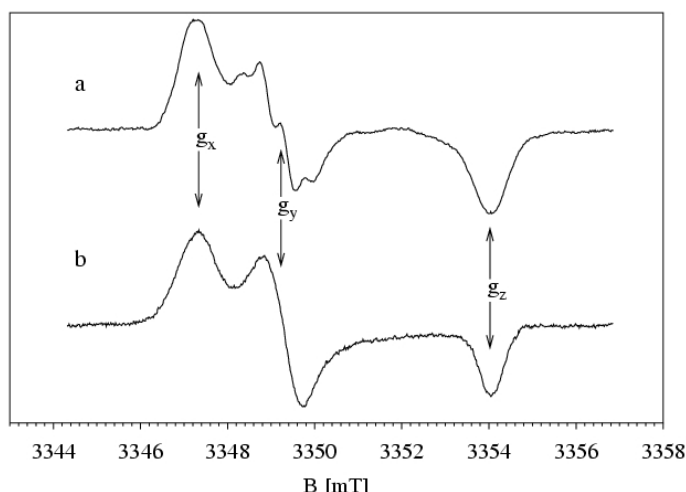
ENDOR accessory. DFT calculations were performed with DGauss for geometry optimizations, Gaussian98 to obtain hyperfine coupling constants (hfc's), and ADF for g tensor calculations. For the DFT calculations the binding pocket of the phylloquinone in the PsaA protein subunit was essentially reduced to three amino acids, i.e. Trp A697, Phe A689, and Leu A722. The phylloquinone phytyl chain was replaced by an ethyl group. The model of the binding site used in the calculations is shown in Fig. 1.

Results

High-field EPR: Figure 2 compares the high-field (94 GHz) EPR spectra of $A_1\dot{-}$ in PS I and of $VK_1\dot{-}$ in DME/MTHF. The g tensor principal values for both species evaluated from the spectra are given in fig. 2. As for other quinones a significant difference of the g anisotropy is obtained between $VK_1\dot{-}$ in the apolar solvent DME/MTHF and in the polar alcohol isopropanol ($g_{x,y,z} = 2.0056, 2.0049, 2.0022$) (Burghaus 1993). A striking coincidence of the complete g tensor of $A_1\dot{-}$ with that of $VK_1\dot{-}$ in DME/MTHF is found. The g tensor for $A_1\dot{-}$ given here from 94 GHz EPR agrees well with data obtained at 283 GHz (MacMillan, 1997).

Fig. 2

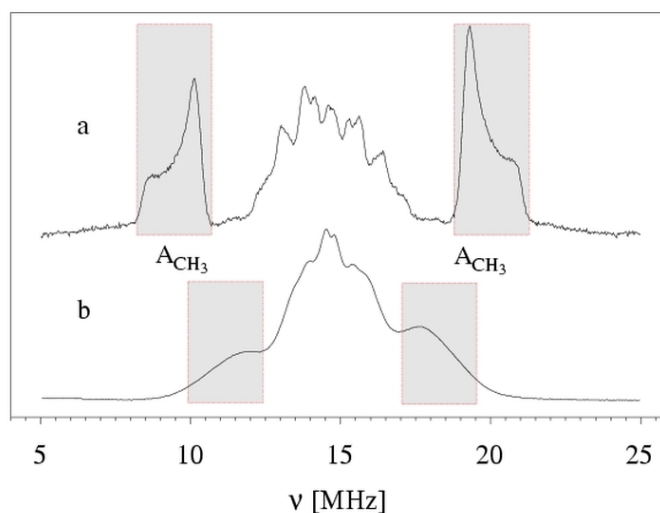
High-field (94 GHz) EPR spectra of a) $A_1\dot{-}$ in PS I ($g_{x,y,z} = 2.00625 / 2.00512 / 2.00220$) and b) $K_1\dot{-}$ in DME/MTHF ($g_{x,y,z} = 2.00623 / 2.00505 / 2.00220$). $T = 80$ K, 0.16μ W, field modulation depth 2G.



ENDOR: The ENDOR spectra of $A_1\dot{-}$ in PS I and $VK_1\dot{-}$ in DME/MTHF are shown in fig. 3. While the corresponding high-field EPR spectra are very similar, indicating identical g tensors, the ENDOR spectra are quite different. As in the case of $VK_1\dot{-}$ in isopropanol, the hfc of the 2- CH_3 group is much smaller for $VK_1\dot{-}$ in DME/MTHF than for $A_1\dot{-}$ in PS I. The isotropic value of this coupling is increased from 7.3 MHz in $VK_1\dot{-}$ to 10.3 MHz in $A_1\dot{-}$. DFT calculations have shown that an increased 2- CH_3 hfc can be caused by strong asymmetric hydrogen bonding to the quinone oxygens (O'Malley 1999).

Fig. 3

Pulse ENDOR (9 GHz) spectra of a) $A_1\dot{-}$ and b) $K_1\dot{-}$ in DME/MTHF. $T = 80$ K, Davies ENDOR, $\pi = 128$ ns, $\pi_{RF} = 8 \mu$ s, $\tau = 600$ ns. The hf tensor range of 2- CH_3 is shaded.



DFT calculations: Here we investigate the influence of the specific protein surrounding of the A_1 binding pocket on calculated magnetic interaction parameters of $A_1\dot{-}$. The model of the A_1 binding site taken from the recent X-ray structure model (Jordan, 2001) shown in Fig. 1 was first geometry optimized with DGauss. The optimized geometry was found compatible with the electron density. With this structure hfc's have been calculated using Gaussian98, and g tensors using ADF. The calculations show that each amino acid in our model leads to a reduction of the g anisotropy approaching the experimental values. For the optimized structure we obtain $g_{x,y,z} = 2.0075, 2.0052, 2.0020$ in reasonable agreement with the experimental values for $A_1\dot{-}$ (2.0063, 2.0051, 2.0022) except for g_x . This could be due to either a deficiency of the theoretical method or the non-optimal model. The hyperfine coupling constant for the 2-CH₃ group in the complete model increases compared to those calculated *in vacuo*. However, the increase is less than experimentally observed for $A_1\dot{-}$. A further increase of the calculated values for this coupling is achieved by shortening the hydrogen bond distance between the oxygen and the NH proton of Leu A722. With the hydrogen bond distance taken as in the optimized structure, an increase of the calculated 2-CH₃ coupling close to the experimental value can also be achieved by a removal of Trp A697 from the model of the binding pocket. This shows that the π -stacking between the Trp A697 and the phylloquinone has a significant influence on the calculated spin density distribution in $A_1\dot{-}$. Other interesting hfc's are those of the backbone nitrogen of Leu A722 involved in the hydrogen bond, the indole nitrogen of Trp A697, and of the proton in the hydrogen bond. It is important to note that the hfc's of the backbone nitrogen and of the proton in the H-bond are virtually identical in presence or absence of Trp A697. The calculated values of these parameters are summarized in table 1. For the proton in the hydrogen bond we calculate a hfc that is somewhat smaller than the experimental value given by (Rigby 1996). It is remarkable that the DFT calculation clearly shows that spin density is

transferred via the H bond to the backbone NH of Leu A722 and also via π -stacking to the Trp. The extent is small but sufficient for a detection by magnetic resonance methods (Hanley 1997).

Table 1 Experimental and calculated hfc of $A_1\dot{-}$ (in MHz)

| | A'_x | A'_y | A'_z | a_{iso} | |
|--------------------------|--------|--------|--------|-----------|--------------------|
| CH ₃ | -1.26 | 2.52 | -1.26 | 10.27 | (Teutloff 1998) |
| | | | | 8.33 | calc. |
| | | | | 9.79 | calc. (w/o W A697) |
| ¹⁴ N peptide | -0.21 | -0.21 | 0.42 | 0.23 | (Hanley 1997) |
| ¹⁴ N Leu A722 | -0.17 | -0.14 | 0.31 | 0.80 | calc. |
| ¹⁴ N Trp | -0.05 | -0.05 | 0.10 | 1.41 | (Hanley 1997) |
| ¹⁴ N Trp A697 | -0.44 | -0.40 | 0.84 | -0.02 | calc. |
| H-bond | -6.4 | -6.4 | 12.8 | 0.6 | (Rigby 1996) |
| H-bond Leu A722 | -4.56 | -4.50 | 9.06 | -0.37 | calc. |

Discussion

The one-sided hydrogen bond to A_1 is reflected in the increased hfc of the 2-CH₃ group of A_1 . The particular sensitivity of the 2-CH₃ to the presence of Trp A697 might be an effect of the geometry optimization of the model for the A_1 binding site. The general spin density asymmetry in $A_1\dot{-}$ is well reproduced by the calculations with the presented model of the A_1 binding site. It is, however, not clear if the spin density shift in $A_1\dot{-}$ is relevant for the function of the quinone in PS I or if it is merely a consequence of the asymmetric binding situation. The high-field EPR shows that the

g anisotropy of A_1^- in PS I is identical to VK_1^- in the apolar solvent DME/MTHF. The g anisotropy can be considered as an indicator for the effective polarity of the environment surrounding the phylloquinone in the A_1 binding site and gives a rationale for the very negative reduction potential of A_1 . This is also based on the finding that the reduction potential is much more negative for VK_1 in the apolar non-protic ether DME/MTHF than in the alcohol isopropanol as preliminary determinations of the redox potentials indicate (Teutloff, unpubl.).

Acknowledgments

This work was supported by Deutsche Forschungsgemeinschaft (Sfb 498; TP A1, A4 and C5) and European Community (FMRX-CT98-0214).

References

- Burghaus O, Plato M, Rohrer M, Möbius K, MacMillan F, Lubitz W (1993) *Journal of Physical* **97**, 7639.
- Hanley J, Deligiannakis Y, MacMillan F, Bottin H, Rutherford AW (1997) *Biochemistry* **36**, 11543.
- Jordan R, Fromme P, Klukas O, Witt HT, Saenger W, Krauß N (2001) *Nature* **411**, 909.
- MacMillan F, Hanley J, van der Weerd L, Knüpling M, Un S, Rutherford AW (1997) *Biochemistry* **36**, 9297.
- O'Malley PJ (1999) *Biochimica et Biophysica Acta* **1411**, 101.
- Rigby SEJ, Evans MCW, Heathcote P (1996) *Biochemistry* **35**, 6651.
- Teutloff C, MacMillan F, Bittl R, Lenzian F, Lubitz W (1998) in *Photosynthesis: Mechanisms and Effects* (G. Garab ed.), Vol. I, p. 607, Kluwer Academic Press, Dordrecht